Layer-resolved kinetics of Si oxidation investigated using the reflectance difference oscillation method

T. Yasuda,[1,2,*] N. Kumagai,[1,3] M. Nishizawa,[1,2] S. Yamasaki,[1,2] H. Oheda,[4] and K. Yamabe[4]
[1]*Joint Research Center for Atom Technology (JRCAT), 1-1-1 Higashi, Tsukuba 305-8562, Japan*
[2]*National Institute of Advanced Industrial Science and Technology (AIST), 1-1-1 Higashi, Tsukuba 305-8562, Japan*
[3]*Angstrom Technology Partnership (ATP), 1-1-1 Higashi, Tsukuba 305-8562, Japan*
[4]*Institute of Applied Physics, Tsukuba University, Tennodai, Tsukuba 305-8573, Japan*
(Received 2 April 2003; published 30 May 2003)

Dry oxidation kinetics of the Si(001) surface has been investigated using reflectance difference oscillation to resolve atomic-scale phenomena. The activation energy for oxidation has been found to increase as the oxide-Si interface moves in the depth direction, reaching the value for bulk oxidation, 2.0 eV, at the third layer from the surface. The nonlinear dependence of the oxidation rate on the O_2 pressure, which was reported for bulk oxidation, has also been observed in the second- and third-layer oxidation. Chemical reaction and mass transport mechanisms for this initial oxidation regime are discussed.

DOI: 10.1103/PhysRevB.67.195338 PACS number(s): 68.35.−p, 78.68.+m, 81.05.Cy, 81.65.Mq

I. INTRODUCTION

The importance of surface oxidation to a broad range of technologies has motivated fundamental studies to ascertain the mechanisms by which oxidation proceeds.[1] Oxidation of Si has received particular attention in recent decades because of its importance to semiconductor device fabrication.[2,3] Present-day metal-oxide-semiconductor devices now require gate insulator films thinner than 2 nm, making it imperative to understand the chemical reactions and mass transport processes in the ultrathin regime. While the classical model developed by Deal and Grove accurately predicts the oxidation rate in the relatively thick regime,[4] oxidation is much faster than their formulation when the thickness is under 30 nm.[5] A number of studies were therefore carried out to bridge this gap,[6–8] resulting in modified kinetic models for this thin regime (2–30 nm).[5,9–11] However, research in the ultrathin regime (<2 nm) has not yet reached the same level of maturity, due to the difficulty in acquiring an unambiguous thickness measurement of ultrathin oxide layers.

This paper addresses the kinetics and mechanisms of Si oxidation in the ultrathin regime. The accuracy of the oxide thickness measurements is critically important to characterize the kinetics in this regime. We employ the reflectance difference (RD) oscillation method[12] to meet this requirement.[13,14] An atomically flat oxide-Si(001) interface, which appears upon complete oxidation of each atomic layer of Si,[15] induces anisotropy in the dielectric response of the Si crystal. Due to the twofold symmetry of the Si layer at the interface, this anisotropy changes its sign each time oxidation proceeds by one atomic layer. Our previous study showed that the RD between two orthogonal polarizations of light indeed oscillates as oxidation proceeds in the depth direction on Si(001), and that each local maximum or minimum of the RD oscillation curve corresponds to the complete oxidation of one atomic layer.[14] Thus, oxidation-rate measurements with atomic-layer resolution are possible by the RD oscillation technique.

Capitalizing on this layer-resolving power, we examine the activation energy and O_2 pressure dependence of the oxidation process for each of the second, third, and fourth layers from the surface. Variation of the activation energy with oxidation depth is observed for the first time, to our knowledge. Surprisingly, some of the major features of the bulk oxidation kinetics appear in the very early stages of oxidation.

II. EXPERIMENT

A. Surface preparation and oxidation procedures

Experiments were performed in an ultrahigh-vacuum chamber equipped with a strain-free window for optical access. The initial Si(001) surface was reconstructed into the singledomain 2×1 structure in order to obtain a nonzero RD amplitude on (001).[16] To prepare the single-domain surface, we used a (001) wafer with an intentional miscut of 4° in the $\langle 110 \rangle$ direction. The wafer was flashed in ultrahigh vacuum at 1470 K for 10 s to form the single-domain surface with the dimer bonds perpendicular to the miscut direction. Sample heating was carried out by flowing a dc current through the Si sample. As oxidation proceeds, reconstruction of the initial surface vanishes but the step structure created by the miscut is preserved [see Fig. 1(b)].

Two protocols were used to oxidize the Si samples that had been flashed and cooled. In the first protocol, hereafter referred to as one-step oxidation, O_2 gas was introduced into the chamber, and its pressure, p_{O_2}, was set to the intended level using capacitance manometers. Two capacitance manometers of different full scales were used to accurately measure p_{O_2} in a wide range from 0.010 to 200 Pa. The first layer of the Si surface was partially oxidized during the p_{O_2} adjustment. After p_{O_2} was stabilized, heating of the sample was started to bring the sample to the target oxidation temperature, T_s. In the second protocol, hereafter referred to as two-step oxidation, the samples were exposed to an O_2 pressure of 0.060 Pa at 1023 K for 1 s, to completely convert the first Si layer into an oxide.[14,15] The second and subsequent layers were then oxidized using various combination of p_{O_2}

 ©2003 The American Physical Society

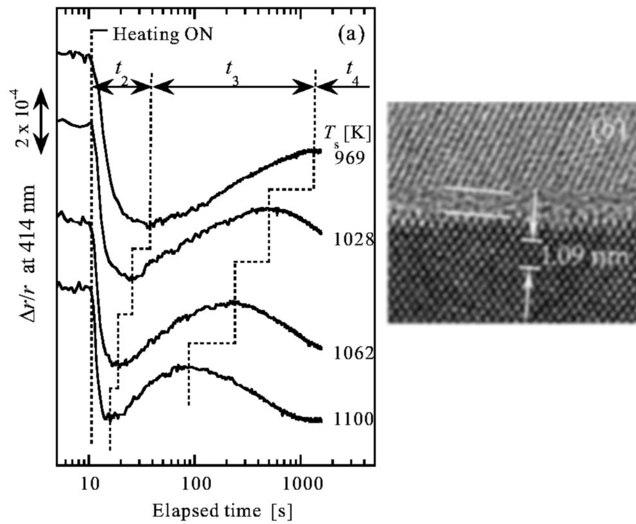

FIG. 1. (a) Examples of RD oscillation curves measured *in situ* during oxidation. p_{O_2} was 0.60 Pa and T_s was varied as noted in the figure. Curves are shown with vertical offsets for clarity. The heating was started at 10 s. Definitions of t_2, t_3, and t_4 are illustrated in the plot. (b) A cross-section TEM image of a 4°-off (001) sample which was oxidized under 0.60 Pa at 1073 K for 120 s. The capping layer on oxide is polycrystalline Si deposited by chemical vapor deposition. Two parallel lines indicate the oxide interfaces.

and T_s. Temperature measurements were made using a pyrometer which we had calibrated by referring to the temperature of $1\times1-7\times7$ phase transition on Si(111), 1113 K.[17] T_s was always set lower than the critical temperature for thermal etching of Si by O_2 (e.g., approximately 1100 K at 0.010 Pa). The base pressure of the vacuum chamber was kept in the 10^{-6}-Pa range even when the sample was heated to 1400 K.

B. RD measurements

The RD amplitude of the sample was measured *in situ* as the initial 2×1 surface was oxidized. In this study, an RD amplitude $\Delta r/r$ is defined as $\Delta r/r=2(r_a-r_b)/(r_a+r_b)$, where r_a and r_b are complex reflectances for polarization parallel and perpendicular to the direction of the dimmer bonds on the initial 2×1 surface, respectively. The optical setup for the RD measurements follows the configuration reported by Aspnes *et al.*[18]

A GaN semiconductor laser (414 nm) was used as the light source in our setup.[19] As we reported previously, the RD spectra of the oxidized surfaces show a main peak near the E_1 transition energy of Si, 3.4 eV at room temperature.[14] When the sample temperature is elevated for oxidation, this peak is supposed to redshift by approximately 0.3 eV.[20] The photon energy of the GaN laser is therefore suitable to monitor the RD change near the main peak position. Preliminary experiments changing the laser output power from 0.05 to 0.5 mW showed that oxidation enhancement by laser irradiation is negligible.

III. RESULTS AND DISCUSSION

A. Observation of layer-by-layer oxidation by RD oscillation

Typical examples of RD oscillation data at 414 nm are shown in Fig. 1(a). The RD amplitude exhibits oscillatory changes once heating is started, and oscillation becomes faster as T_s is increased. Data are presented on a logarithmic time scale because the RD change becomes slower with the oxidation time, making detection of the peaks harder on a plot using a linear time scale. According to the spectral measurement that we reported previously,[14] complete oxidation of the first layer of Si should produce a maximum in the RD trace. However, this is not discernable in Fig. 1(a) because the first-layer oxidation was completed in a very short time (<1 s) after the heating was started. The first observable peak in the RD amplitude is a local minimum, shown at an elapsed time of 15–40 s in Fig. 1(a). At this point, oxidation of the second layer from the surface has just completed. The half period t_2, as defined in the plot, is the time required to complete the second-layer oxidation. As oxidation continues, the RD amplitude next reaches a local maximum, which indicates complete oxidation of the third layer. t_3, as shown in Fig. 1(a), is the time required to fully oxidize this third layer. Complete oxidation of the fourth layer and beyond is determined similarly to t_2 and t_3.

Figure 1(b) shows a cross-section transmission electron microscopy (TEM) image of the sample oxidized at 0.60 Pa and 1072 K for 120 s. According to Fig. 1(a), three layers of Si have been oxidized at this condition. Since approximately 0.3 nm of oxide is formed by oxidation of one layer on Si(001),[2] the expected thickness of oxide is 0.9 nm. As seen in Fig. 1(b), the thickness indeed measures approximately 0.9 nm. The measurement error, however, may be as large as the thickness of one monolayer of Si crystal due to ambiguity in defining the oxide interfaces.

We observed that the RD amplitude oscillates more clearly at higher p_{O_2}. For instance, an unambiguous measurement of t_3 was often difficult when p_{O_2} was lower than 0.060 Pa. On the other hand, an oscillation up to the sixth-layer oxidation was observed in some runs at 200 Pa. At p_{O_2} above 20 Pa, however, the Ta electrodes for resistive heating were severely oxidized, so the reproducibility of the oscillation data was not satisfactory for detailed investigation of kinetics.

B. Layer-resolved determination of the activation energy

We have acquired more than eighty traces of RD oscillation to measure t_i ($i=2$, 3, and 4) for various combinations of T_s and p_{O_2}. Data for t_i are plotted in the Arrhenius form in Figs. 2(a)–2(d). The former two figures are for t_2, and the latter two are for t_3 and t_4. The following regression line is fit to each data set acquired at constant p_{O_2}:

$$1/t_i=C_i\cdot\exp(-\Delta E_i/kT_s), \tag{1}$$

where k is the Boltzman constant. ΔE_i is the energy barrier for the rate-governing process for the ith layer oxidation.

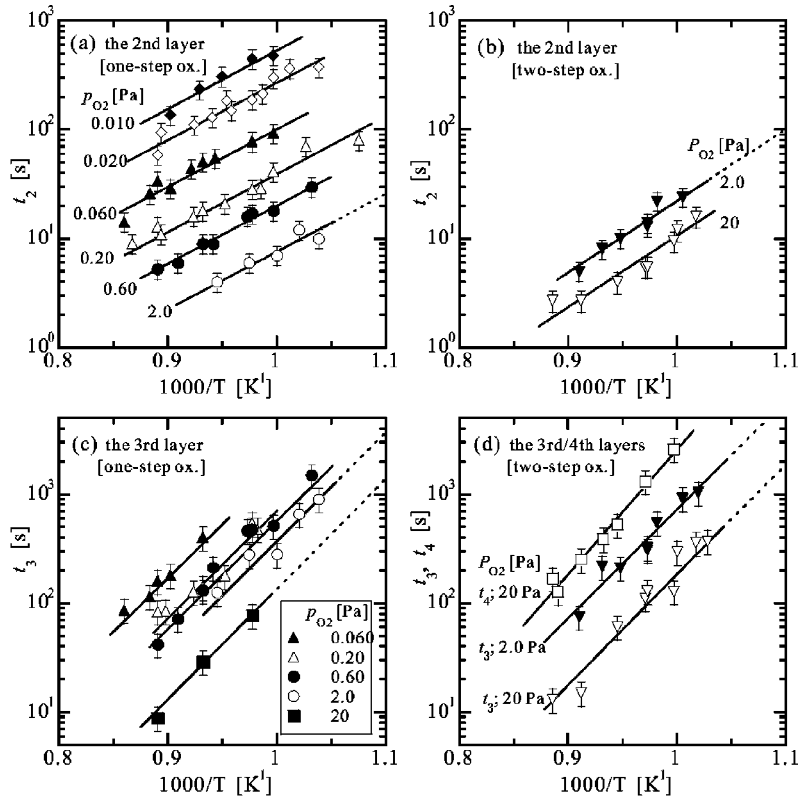

FIG. 2. Arrhenius plots for t_2, t_3, and t_4 measured at various p_{O_2} levels. (a) t_2 by one-step oxidation. (b) t_2 by two-step oxidation. (c) t_3 by one-step oxidation. (d) t_3 and t_4 by two-step oxidation. The p_{O_2} conditions are indicated in the plots.

The pre-exponential factor, C_i, is a function of p_{O_2}, but its explicit expression is open at present.

Data and regression lines for the second-layer oxidation using the one-step protocol is given in Fig. 2(a) for six different p_{O_2} conditions. As the figure shows, the slopes of the regression lines are identical, indicating that ΔE_2 is independent of p_{O_2}. ΔE_2 is estimated to be 1.1 ± 0.2 eV.

When p_{O_2} was higher than 0.6 Pa, we noticed that the first-layer oxidation was nearly complete at room temperature during the p_{O_2} adjustment at the beginning of an oxidation run. In order to investigate whether t_2 is affected by the condition of the first-layer oxidation, we carried out oxidation using the two-step protocol. The Arrhenius plot for the two-step runs is shown in Fig. 2(b). A comparison between the 2.0 Pa data in Figs. 2(a) and 2(b) shows that t_2 becomes longer (approximately $\times 4$ as shown by dotted extension of the regression lines) if the first-layer oxidation has been completed at an elevated temperature by the two-step process. ΔE_2 for Fig. 2(b) is 1.3 ± 0.2 eV, which is only slightly larger than that for Fig. 2(a). This *aftereffect* of the first-layer oxidation temperature on the second-layer oxidation rate will be discussed in the last part of this article.

Figures 2(c) and 2(d) show the data and regression lines for the third-layer oxidation using the one- and two-step protocols, respectively. ΔE_3 is again independent of p_{O_2}, and is estimated to be 2.0 ± 0.2 eV for both protocols. Compared to the second-layer oxidation, t_3 is less sensitive to whether oxidation was performed in one or two steps.

Reliable data for t_4 were obtained at relatively high p_{O_2} of 20 Pa, as the RD amplitude oscillated clearer and longer at higher p_{O_2}. As shown in Fig. 2(d), ΔE_4 is estimated to be 2.2 ± 0.2 eV, which is essentially equal to the value for the third-layer oxidation.

ΔE_i values determined from Fig. 2 are tabulated in Table I along with the activation energies reported in the literature. An examination of ΔE_i values for the first, second, and third layers shows that ΔE_i monotonically increases as oxidation proceeds in the depth direction, reaching to 2.0 eV at the third layer. Kato *et al.* revealed by an *ab initio* calculation that the first layer of the 2×1 Si(001) surface is oxidized without any energy barrier as oxygen atoms in the chemisorbed state migrate into the backbond center position.[21,22] For the second layer oxidation, Watanabe *et al.* reported ΔE_2 of 0.3 eV.[15] This value is much smaller than those determined in Figs. 2(a) and 2(b). In their experiments, the rate of the second-layer oxidation was estimated by measuring the initial increase of the O *KLL* Auger electron intensity with time. Therefore, the ΔE_2 value in Ref. 15 is for the *initial* stage of the second-layer oxidation. On the other hand, ΔE_2

TABLE I. Variation of ΔE_i with progression of oxidation in the depth direction.

Layer to be oxidized	ΔE_i (eV)	p_{O_2} (Pa)	Ref.
$i=1$	0		21
2[a]	0.3	$\sim10^{-4}$	15
2	1.2 ± 0.3	$0.01\sim20$	this work
3	2.0 ± 0.2	$0.06\sim20$	this work
4	2.2 ± 0.2	20	this work

[a]Initial stage.

determined from t_2 in Figs. 2(a) and 2(b) is for completion of the second-layer oxidation. More specifically, because the RD change becomes slower with progression of oxidation, ΔE_2 determined from the RD oscillation is for the *late* stage of the second-layer oxidation. Thus, these two ΔE_2 values also indicate that the activation energy increases as oxidation progresses. The oxidation of the second and subsequent layers should be associated with structural changes in the already formed oxide network which are likely to cause an increase in ΔE_i.[22]

A number of studies have reported activation energies for the oxidation reaction at the oxide-Si interface when the oxide thickness is greater than 2 nm.[6] Reported energies range from 1.5,[23,24] 1.9,[25] and 2.0 eV,[4,10,26] to 2.4 eV.[5] It has also been argued that the activation energy varies with the thickness regime.[5,25,27] Disagreement among the past studies is mainly due to the fact that different values of the activation energy may be deduced if different kinetic models are employed for data analyses.[11,28] Another factor to be considered in the thickness regime less than 10 nm is the error in the ellipsometric thickness measurements.[29] In the present study, ΔE_i estimation does not suffer from either the model dependence or the error in the thickness measurement, because ΔE_i is estimated directly from the layer-resolved measurements of t_i.

ΔE_3 and ΔE_4 values in Table I are near or slightly higher than the median of the variation range mentioned above: 1.5–2.4 eV. This suggests that the chemical process that governs the interface reaction in the thicker regime begins with oxidation of the third layer from the surface.

The reported activation energy has been often compared to the energy needed to break the Si-Si bond energy, 1.83 eV. Recent studies suggest that the rate-limiting step is not the reaction between O_2 and Si-Si bonds, but the generation of the so-called reactive sites. The layer-resolved activation energies obtained in this study are expected to be the critical test to identify what process governs the oxidation reaction at the interface.

We point out that, since reduced ΔE_i only contributes to the first- and second-layer oxidation, the main cause for fast oxidation from the third layer through the thin (2–30 nm) regime is not ΔE_i reduction near the surface. Instead, the fast oxidation should be ascribed mainly to the larger availability, or chemical activity, of oxidants than those predicted by the conventional dissolution-diffusion mechanism.[4,5] As for the ultrathin regime, one of the possible mechanisms of the large availability of O_2 is the ballistic transport through SiO_2. According to the recent quantum molecular dynamics calculation,[30] the ballistic path contributes to oxidation at least when oxide thickness is 0.7 nm or less.

C. Nonlinear dependence of the oxidation rate on oxygen pressure

Figure 3 plots the dependence of C_2 and C_3 on p_{O_2}. C_2 and C_3 were calculated according to Eq. (1) for each regression line in Fig. 2. For the one-step oxidation process, C_2 and C_3 are proportional to $p_{O_2}{}^{0.79}$ and $p_{O_2}{}^{0.43}$, respectively.

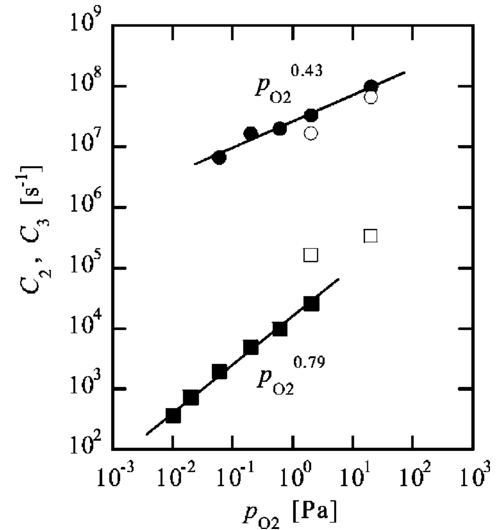

FIG. 3. Dependence of C_2 and C_3 on p_{O_2}. Filled and open squares are for C_2 obtained from the regression lines in Figs. 2(a) and 2(b), respectively. Filled and open circles are for C_3 obtained from Figs. 2(c) and 2(d), respectively.

Here it should be reminded that, in the one-step procedure, the effective temperature for the first-layer oxidation was lower at higher p_{O_2}, as mentioned in Sec. III A. When the first layer is oxidized at a lower temperature, the oxidation of the second layer becomes faster as shown in Figs. 2(a) amd 2(b). If we take this effect into account, the real dependence of C_2 on p_{O_2} is thought to be weaker than the apparent one in Fig. 3. In Fig. 3, the two data points of C_2 by the two-step oxidation indeed show a dependence weaker than $p_{O_2}{}^{0.79}$, though the number of the data points is not sufficient to determine the exact order.

Observed nonlinear dependence of C_i on p_{O_2} provides us with further insight into the microscopic mechanism of the oxidation reaction. The observed nonlinear dependence is presumably related to the nature of the chemical reaction at the oxide-Si interface, rather than the mass transport process, since the transport rate is essentially linear with p_{O_2}. The linear rate constant in the Deal-Grove model is proportional to $p_{O_2}{}^{0.7} - p_{O_2}{}^{0.8}$ at both reduced (10^3–10^5 Pa) (Refs. 5 and 31) and high (10^6–10^8 Pa) (Ref. 32) pressures. In contrast, the wet oxidation rate is linear with the H_2O pressure.[33] Recent Monte Carlo simulation showed that the oxidation rate by oxygen *atoms* is also linear with the chemical potential of the oxygen atoms.[34] Thus, the nonlinear dependence on p_{O_2} is an essential character of the chemical interaction between O_2 molecules and Si at the interface.

So far, only a few models have succeeded in simulating the dependence of the linear rate constant on p_{O_2}.[11,35] In general, sublinear rate processes are explained by postulating the reaction intermediates or inhibitors that are generated in the reaction system. Uematsu *et al.* reported that the dry oxidation rate at various p_{O_2} can be well simulated by considering emission of Si atoms from the interface.[35] They assumed that the emitted Si atoms near the interface inhibit the

oxidation reaction. Further examination is needed as to whether a similar model can explain the oxidation rate in the ultrathin regime.

D. Effects of structures of the initial Si surface and oxide layer on subsequent oxidation

Now we discuss the aftereffect observed in Figs. 2(a) and 2(b). As mentioned above, the second-layer oxidation becomes slower if the first-layer oxidation is executed at an elevated temperature. The observed decrease (e.g., a factor of 4 at 2.0 Pa) is perhaps too large to be ascribed to a change in O_2 transport through only a single layer of oxide. Recent studies suggest that the rate-limiting chemical process at the oxide-Si interface is generation of the so-called reactive sites or Si-containing entities to be oxidized.[36,37] The observed aftereffect may imply that such chemical processes are affected by the structure and property of the oxide layer(s) that had already been formed.

In general, the oxidation rate of the ith Si layer may be affected by the structure of the $(i-1)$th and preceding oxide layers. However, for the t_3 and t_4 data shown in Figs. 2(c) and 2(d), this effect is assumed to be minor. Compared to the 750 K temperature difference in the first-layer oxidation between the one- and two-step protocols, the T_s variation for the second- and third-layer oxidation is relatively small at only 130 K.

Related to the aftereffect discussed above, it was observed that oscillation periods on the on-axis (001) face, which was made single domain by the electromigration technique, were essentially the same as those shown in Fig. 2.[14,19] We also compared the oxidation rates between the single- and double-domain surfaces for selected oxidation conditions. Analyses by Auger electron spectroscopy showed that the oxidation rates are almost the same between the two kinds of the surfaces. These observations imply that neither singularity of the domain structure nor the terrace width affects the oxidation rate. Instead, we have found that hydrogen termination of the initial surface, which should lead to the incorporation of Si-H and Si-OH bonds in the oxide layer and thereby alter its network structure, significantly retards the oxidation process. The effect of hydrogen termination on the oxidation rate is an important issue from the application point of view and will be discussed in a separate report.

IV. SUMMARY

Oxidation kinetics of the 2×1-Si(001) surface was investigated with atomic layer resolution by utilizing reflectance-difference oscillation. We showed that the activation energy increases as oxidation proceeds, converging to the value for the bulk oxidation at the third layer from the surface. The sublinear dependence of the oxidation rate on p_{O_2} was observed for the second- and third-layer oxidation. The condition of the first-layer oxidation was found to affect the oxidation rate of the second layer. It is our hope that the layer-resolved kinetic data presented in this paper will serve as a base to understand the mechanisms of interface evolution and associated defect generation processes.

ACKNOWLEDGMENT

We thank Ronald Kuse for his assistance in finalizing the manuscript. This study was partly supported by NEDO.

*Electronic address: yasuda-t@aist.go.jp

[1] N. Cabrera and N.F. Mott, Rep. Prog. Phys. **12**, 163 (1949).
[2] E. H. Nicollian and J. R. Brews, *MOS (Metal Oxide Semiconductor) Physics and Technology* (Wiley, New York, 1982), p. 647.
[3] *Fundamental Aspects of Silicon Oxidation*, edited by Y. J. Chabal (Springer, Berlin, 2001).
[4] B.E. Deal and A.S. Grove, J. Appl. Phys. **36**, 3770 (1965).
[5] H. Massoud, J.D. Plummer, and E.A. Irene, J. Electrochem. Soc. **132**, 2685 (1985).
[6] J. D. Plummer, in *The Physics and Chemistry of SiO_2 and Si-SiO_2 Interface 3*, edited by H. Z. Massoud, E. H. Poindexter, and C. R. Helms (Electrochemical Society, Pennington, NJ, 1996), p. 129.
[7] M.L. Green, E.P. Gusev, R. Degraeve, and E.L. Garfunkel, J. Appl. Phys. **90**, 2057 (2001).
[8] I.J.R. Baumvol, Surf. Sci. Rep. **36**, 1 (1999).
[9] A. Reisman, E.H. Nicollian, K.C. Williams, and C.J. Merz, J. Electron. Mater. **16**, 45 (1987).
[10] S. Dimitrijev and H.B. Harrison, J. Appl. Phys. **80**, 2467 (1996).
[11] R.M.C. de Almeida, S. Goncalves, I.J.R. Baumvol, and F.C. Stedile, Phys. Rev. B **61**, 12 992 (2000).
[12] D.E. Aspnes and A.A. Studna, Phys. Rev. Lett. **54**, 1956 (1985).
[13] T. Nakayama and M. Murayama, Appl. Phys. Lett. **77**, 4286 (2000).
[14] T. Yasuda, S. Yamasaki, M. Nishizawa, N. Miyata, A. Shklyaev, M. Ichikawa, T. Matsudo, and T. Ohta, Phys. Rev. Lett. **87**, 037403 (2001).
[15] H. Watanabe, K. Kato, T. Uda, K. Fujita, M. Ichikawa, T. Kawamura, and K. Terakura, Phys. Rev. Lett. **80**, 345 (1998).
[16] T. Yasuda, L. Mantese, U. Rossow, and D.E. Aspnes, Phys. Rev. Lett. **74**, 3431 (1995).
[17] K. Tsukui, K. Endo, R. Hasunuma, O. Hirabayashi, N. Yagi, H. Aihara, T. Osaka, and I. Ohdomari, Sci. Sin. **328**, L553 (1995).
[18] D.E. Aspnes, J.P. Harbison, A.A. Studna, and L.T. Florez, J. Vac. Sci. Technol. A **6**, 1327 (1988).
[19] T. Matsudo, T. Ohta, T. Yasuda, M. Nishizawa, N. Miyata, S. Yamasaki, A. Shklyaev, and M. Ichikawa, J. Appl. Phys. **91**, 3637 (2002).
[20] J. Sik, J. Hora, and J. Humlicek, J. Appl. Phys. **84**, 6291 (1998).
[21] K. Kato, T. Uda, and K. Terakura, Phys. Rev. Lett. **80**, 2000 (1998).
[22] K. Kato and T. Uda, Phys. Rev. B **62**, 15 978 (2000).
[23] E.A. Irene and Y.J. van der Meulen, J. Electrochem. Soc. **123**, 1380 (1976).
[24] P. Thanikasalam, T.K. Whidden, and D.K. Ferry, J. Vac. Sci. Technol. B **14**, 2840 (1996).
[25] C.J. Han and C.R. Helms, J. Electrochem. Soc. **134**, 1297 (1987).
[26] S.A. Ajuria, P.U. Kenkare, A. Nghiem, and T.C. Mele, J. Appl. Phys. **76**, 4618 (1994).
[27] S. Kamohara and Y. Kamigaki, J. Appl. Phys. **69**, 7871 (1991).

[28] J. Blanc, Philos. Mag. B **25**, 685 (1987).
[29] E.A. Irene, Solid-State Electron. **45**, 1207 (2001).
[30] A.A. Demkov and O.F. Sankey, Phys. Rev. Lett. **83**, 2038 (1999).
[31] Y. Kamigaki and Y. Itoh, J. Appl. Phys. **48**, 2891 (1977).
[32] C. Camelin, G. Demazeau, A. Straboni, and J.L. Buevoz, Appl. Phys. Lett. **48**, 1211 (1986).
[33] R.R. Razouk, L.N. Lie, and B.E. Deal, J. Electrochem. Soc. **128**, 2214 (1981).
[34] Y. Tu and J. Tersoff, Phys. Rev. Lett. **89**, 086102 (2002).
[35] M. Uematsu, H. Kageshima, and K. Shiraishi, J. Appl. Phys. **89**, 1948 (2001).
[36] A.M. Stoneham, C.R.M. Grovenor, and A. Cerezo, Philos. Mag. B **55**, 201 (1987).
[37] H. Kageshima and K. Shiraishi, Phys. Rev. Lett. **81**, 5936 (1998).